Graph Based Classification of MRI Data Based on the Ventricular System

S. Seth Long and Lawrence B. Holder
Washington State University

***Abstract*—The ventricular system inside the brain is known to enlarge and change shape given conditions such as Alzheimer's disease. This change in shape may provide a way to assess the level of cognitive impairment of a patient, as well as other intellectual characteristics. This paper describes the use of trees to represent the 3D space containing the third and lateral ventricles, and classification of these trees using frequent subgraph mining and support vector machines. Level of cognitive impairment and years of education are shown to be predictable given a tree representation of the shape of the third and lateral ventricles, demonstrating that the shape of the ventricular system correlates with these attributes. These results were generated using a cross-sectional collection of 416 MR images of subjects ranging in age from 18 to 96 years, including 100 subjects diagnosed with Alzheimer's disease.**

I. Introduction

Many personality traits and talents are reflected in the physical structure of the brain. Likewise, events throughout a person's life can also leave a physical mark on the brain, whether head impacts, drug use, high levels of cognitive use or disuse, high blood pressure, stress, or disease. Many of these physical changes can be observed in an MR image of the brain.

Human involvement in analysis of MR images is a useful diagnostic tool in many cases. However, applying automation to analysis of medical image data allows examination of larger datasets at lesser cost in terms of human time. This reduced cost enables searching for patterns for which adequate justification cannot be found for a time-intensive manual perusal of the data. [1] describes a number of methods which have been applied to automatic brain image analysis.

Analyzing the shape of structures in the brain can be a particular challenge due to lack of clear, defined boundaries around many of them, as noted in [2]. However, the ventricular system provides a sharp contrast to the rest of the brain, appearing dark in color in MR images due to the cerebrospinal fluid inside the ventricles. This provides a natural target for automatic analysis.

The volume of the ventricular system has been shown to increase with the progression of Alzheimer's disease [2]. As such, given a large number of MR images showing the ventricular system, it may be possible to develop an automatic system to determine with some degree of accuracy which images are from patients displaying some level of cognitive impairment. Such a system could use the shape of the ventricular system as well as simple volume in order to form a more accurate representation of the difference between categories.

Given a classifier which can, given two sets of MR images, form a method to distinguish between them based on ventricular shape, it is possible to test if a particular intellectual characteristic correlates with ventricle shape. A reasonable test of such a system is to determine if it can differentiate between cognitively-impaired and healthy individuals, because ventricular volume is known to increase given progression of Alzheimer's disease [2]. See Figure 1 for an example of ventricular enlargement.

This paper describes a method of creating a tree representing the 3D shape of the third and lateral ventricles, by both the tree structure and node and edge labels. Trees created by this method are then classified by finding frequent subtrees which are present only in trees derived from cognitively-impaired or healthy brains. Feature vectors are constructed for each image by presence or absence of the frequent subtrees, and the image is classified by a support vector machine operating on these feature vectors. The hypothesis that such a system should be capable of distinguishing with better than random accuracy between cognitively-impaired and healthy individuals is tested and found to be true, with an accuracy of 72% when mildly impaired individuals (CDR 0.5) are excluded from the test, and 66.3% when they are included.

The system is then used to find a correlation between ventricular shape and level of education, demonstrating 77.2% accuracy classifying highly-educated individuals vs. individuals with no college education. This demonstrates that the system presented in this paper is capable of general-purpose classification provided some physical pattern exists which can be found in the shape of the third and lateral ventricles. This validates the shape-recognition algorithm, indicating it may be suitable as a component of a more general MRI classification system.

II. Previous Work

A. Graph Classification

Graph classification generally relies on either direct comparison between graphs, or by examining frequent substructures within a graph. In [3], the Subdue system is used to distinguish between two classes of graphs by finding a substructure common to most positive examples but few negative examples. It is capable of using multiple subgraphs in order to cover a set of positive examples which may not all have exactly the same substructure in common, but yet some set of defining characteristics does exist.

It is also possible to discover substructures using a frequent subgraph miner, and then use them to create a feature vector to

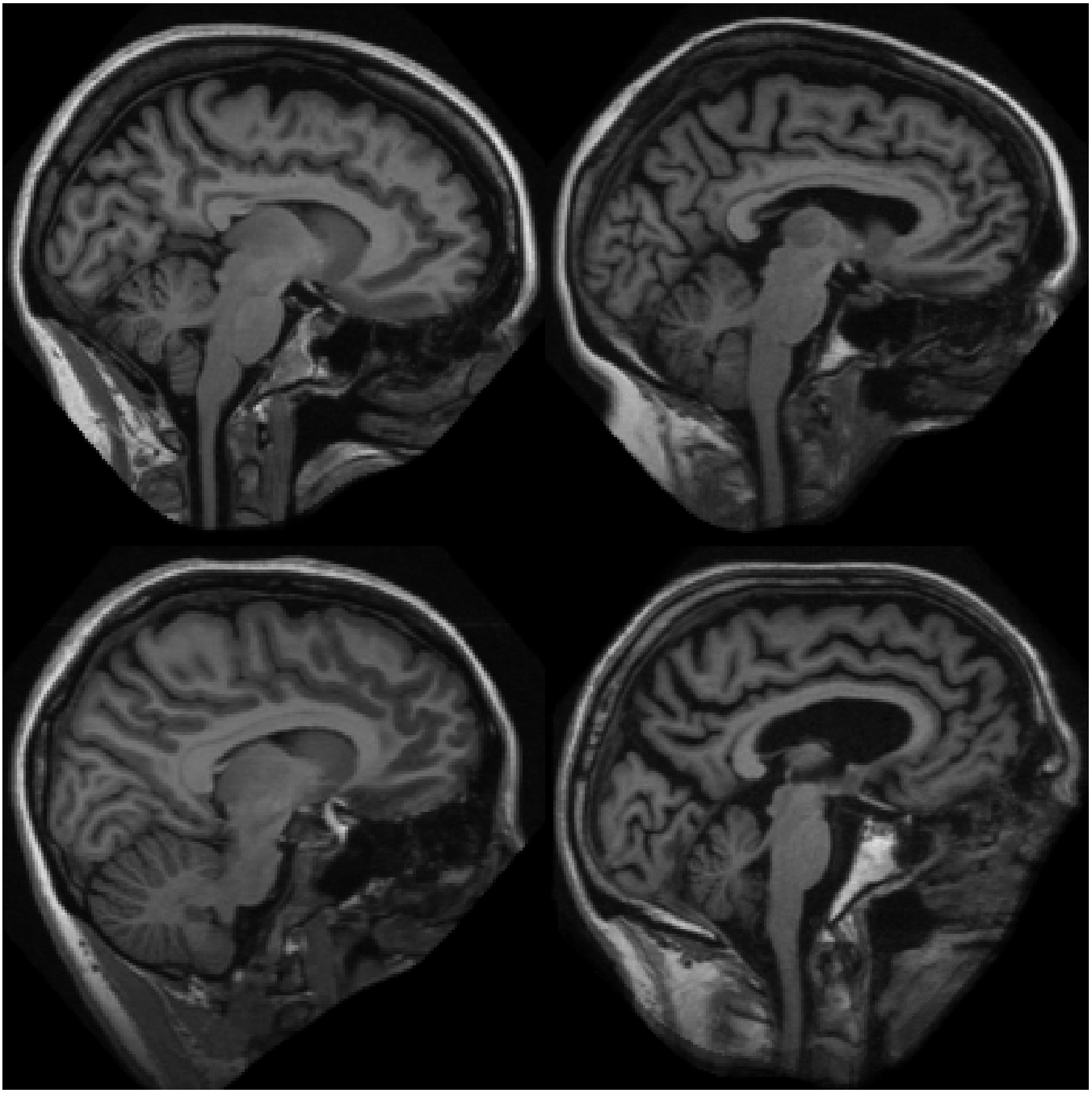

Fig. 1. Left: Saggital images from healthy (CDR 0) brains. Right: Images from patients exhibiting CDR 2. Note enlarged third ventricle, and overall reduced brain volume.

describe a graph. Deshpande et al. use this approach to classify chemical compounds in [4]. Using feature vectors in this manner allows use of more common data mining techniques for classification.

Besides reliance on substructures, it is possible to compare graphs directly. In [5] an SVM kernel is created which directly compares graphs. This avoids costly subgraph isomorphism calculations and can in some circumstances improve accuracy. However, the running time of the graph kernel is long, particularly with large graphs, and it proved computationally infeasible on the graphs used in this paper.

In [6], we test both approaches plus a nearest neighbor approach in an ensemble to classify graphs representing movements of inhabitants of an apartment, with the result that although there is some degree of overlap between the methods, both may also classify certain examples correctly when the other does not.

B. 3D Shape Representation by Graphs

3D graph-based object classification has been done, as in [7], by forming a graph consisting of derived attributes. For example, in [7], Joshi and Chang use shape features such as

edges, etc. to form a graph-based representation of machined features. Similar methods in 2D are also used, for example in [8]. 3D classification is an extension of 2D classification, which has been done in similar ways to that in this paper, for example by Elsayed et al. in [9].

C. Classification of MRI and fMRI images

In [9], Elsayed et al. perform analysis on the shape of the corpus callosum in order to classify brain scans of musicians vs. non-musicians. As a preliminary step, image algorithms are applied to increase the contrast of the corpus callosum, a bounding box is determined for the corpus callosum, and the image is cropped accordingly. After the image is cropped, it is converted into a quad-tree by separating the image into 4 quadrants, then recursively subdividing each quadrant until the image to be subdivided is sufficiently homogeneous (95% uniform in color). Each division forms a branch in the quad-tree, and each non-subdivided image becomes a leaf. This tree then represents the shape of the corpus callosum. Frequent subtrees are found in the set of quad-trees, weighted to give nodes near the root greater weight. A feature vector is produced based on the presence or absence of each frequent subtree and classification is performed using the C4.5 decision tree algorithm. The result is a best classification accuracy of 95.28%, depending on the support threshold for frequent subtrees. This work was extended to include time-series data classification in [10]

In [11], Mitchell et al. use each voxel as a feature, and classify thoughts using machine learning techniques. This is a different though related problem, because this approach is tailored for fMRI data, which is a time sequence of activation, rather than only a static (structural) image of the brain. Feature selection is used to select voxels which are particularly predictive for each task. The total size of the dataset is small, but machine learning is nevertheless demonstrated.

III. Publicly Available MRI Data

Data is available from OASIS [12]. This is a dataset consisting of over 400 MR images, some of individuals with varying levels of cognitive impairment. They are labeled according to the degree of cognitive impairment due to Alzheimer's disease. The data is in the Mayo Clinic Analyze 7.5 format [1]. The Nipy library can be used to access this data from Python code [13].

IV. Graph-Based Shape Classification

A. Finding the Extent of the Third Ventricle

The third ventricle is surrounded primarily by white matter, which forms an obvious contrast to the cerebrospinal fluid inside the ventricle itself. Automatically detecting the ventricles can be done by selecting the portion of the 3D images which is dark in color, or has a low intensity value. This leads to an algorithm expanding the selected area in 3D space, as shown in algorithm 1.

[1] http://www.grahamwideman.com/gw/brain/analyze/formatdoc.htm

Fig. 2. Third and lateral ventricles, post-discovery. From the image, it appears that the full left lateral ventricle may not have been discovered. This is not a problem provided the bounding box containing the third and lateral ventricles is correct. Also, many of the images exhibit asymmetry between the lateral ventricles. The approximate ventricular volume can be obtained based on the number of voxels in the ventricles.

Algorithm 1: Expansion in 3D algorithm
Input: Point p inside III ventricle, intensity threshold T_i
Output: Set of points inside III ventricle
(1) $P \leftarrow [p]$
(2) $C \leftarrow$ Neighbors of p
(3) **foreach** $c \in C$
(4) **if** $c \notin P$ **and** intensity(c) $\leq T_i$
(5) Add c to P
(6) Add Neighbors of c to C
(7) **return** P

The third ventricle is connected to the rest of the ventricular system, and to the spinal canal. The 3D expansion algorithm cannot be allowed to leave the ventricular system and expand to select the spinal canal, which will reach the edge of the MR image and lead to selection of 3D space outside the brain. In general, small passageways in the brain, despite containing CSF, are of higher intensity than the space inside the third ventricle, and therefore some threshold generally exists which will allow the 3D expansion algorithm to select the entire third ventricle and both lateral ventricles without expanding beyond it.

Additionally, the selected area must not extend too far from a known point in the ventricles. In our testing, most images were found to have a suitable threshold. This does require a

known point inside the ventricles. This was provided by human input, but further work could enable automation of this step as well. A user interface was created to allow a point within the ventricles to be specified in only two mouse clicks per image. Marking a point inside one of the lateral ventricles was found to be fastest.

If the image of the brain was a perfect representation, there would be nothing to stop the 3D expansion algorithm from following the cerebral aqueduct completely out of the brain, however in practice MR images record the cerebral aqueduct as lighter than the rest of the ventricular system, providing a stopping point for the algorithm. However, with too low of intensity threshold, the expansion algorithm will not move from one lateral ventricle to the other, stopping either before reaching the third ventricle, or before entering the other lateral ventricle.

Selection of an appropriate intensity threshold was done by automatic trial and error. Progressively higher intensity thresholds are tested until the discovered area is:

1) Balanced evenly on the left and right sides of the brain
2) Of suitable size to potentially include both lateral ventricles

This process can be completed on the entire OASIS dataset using 4 threads on an Intel Q6600 in about two days. Some variance in balance must be allowed given the variability of the human brain. Figure 2 gives an example of the third and lateral ventricles after selection.

B. Derivative of Intensity to Highlight Boundaries

In some cases, appropriate intensity threshold cannot be found without image enhancement. In order to amplify the contrast between white matter and the interior of the third ventricle, edges were highlighted by changing the intensity value to the maximum difference in intensity between a voxel and it's 6 non-diagonal neighbors. This is equivalent to the rate of change in intensity over change in the x, y, or z direction. Using this technique, a total of 387 out of the 416 OASIS images were found to have a suitable intensity threshold, including 27 of 30 images involving a CDR of 1.0 or higher. Figure 3 illustrates the results of this process. The entire recoloration takes around 20 minutes to complete, single-threaded, on an Intel Q6600.

C. Oct-Tree Graph Representation

Once the entire third ventricle is selected, the extent of it can be determined in X, Y, and Z directions. The volume is also determined at this point, although at present this value is not used for classification. The reference points established by the edges of the ventricular system are used to generate the tree. This avoids any particular dependence on voxels, similar to the "anchor points" described by Megalooikonomou et al. in [1].

The area containing the third ventricle is repeatedly subdivided until either the intensity is sufficiently homogeneous over the entire subdivision, or the depth limit for the tree is reached. Subdivision is always into 8 parts, with all parts of equal size forming a 2x2x2 grid. A tree is constructed by representing each subdivision. Reaching a stopping condition causes a leaf in the tree.

D. Labeling

The tree must incorporate spatial information, the graph must include which physical location a branch corresponds to. This is done using edge labels. Also, the condition under which leaves were formed must be recorded (depth limitation, homogeneous dark area, homogeneous white area). Nodes are labeled according to the following scheme:

root	indicates the root node, i.e. the box representing the extent of the ventricles
U	indicates a node which branches into 8 subdivisions
I	indicates a leaf due to depth limitation
W	indicates a leaf due to homogeneous white color
D	indicates a leaf due to homogeneous dark color

Edges are labeled from 0 through 7 depending on which subdivision they represent. Specifically:

- Edges 0-3 indicate subdivisions from the right half of the box
- 4-7 are from the left half
- 0, 1, 4, and 5 are from the inferior (lower) half
- 2, 3, 6, and 7 are from the superior (upper) half
- 0, 2, 4, and 6 are from the rostral (rear) half
- 1, 3, 5, and 7 are from the caudal (front) half

This allows a subgraph to indicate that a particular area must be dark, light, or indeterminate. As such, they can completely represent shape given an adequate number of nodes.

Adjusting the tree depth limit and maximum allowable intensity variance, changes the size of the generated tree. A greater number of nodes provides a more accurate shape representation, but increases computational time. Many common graph operations scale badly relative to the number of nodes, making this a particularly important parameter.

V. Classification of Graphs

Finding a set of subgraphs can be done using a frequent subgraph miner such as Gaston [14] or Gspan [15]. These will, given a set of graph transactions, return all subgraphs more frequent than a given support threshold. In order to represent each of two categories, the training set can be split between negative and positive examples, and the subgraph miner can be run on each of the resulting sets. This was done in [6] for frequent subgraph classification. Splitting the training set in this manner allows subgraphs which are distinct to one classification or the other to be discovered.

Given that trees representing the 3D shape of the ventricular system are all somewhat similar, there is a large amount of overlap between trees representing ventricles from highly-impaired individuals and those from healthy individuals. Also, because a large amount of similarity exists within each category, many frequent subgraphs can be found. Attempts to use Gaston to find useful frequent subgraphs resulted in an overwhelming flood of subgraphs with no particular relevance for classification. Using a set of 27 trees, 12 gb of frequent

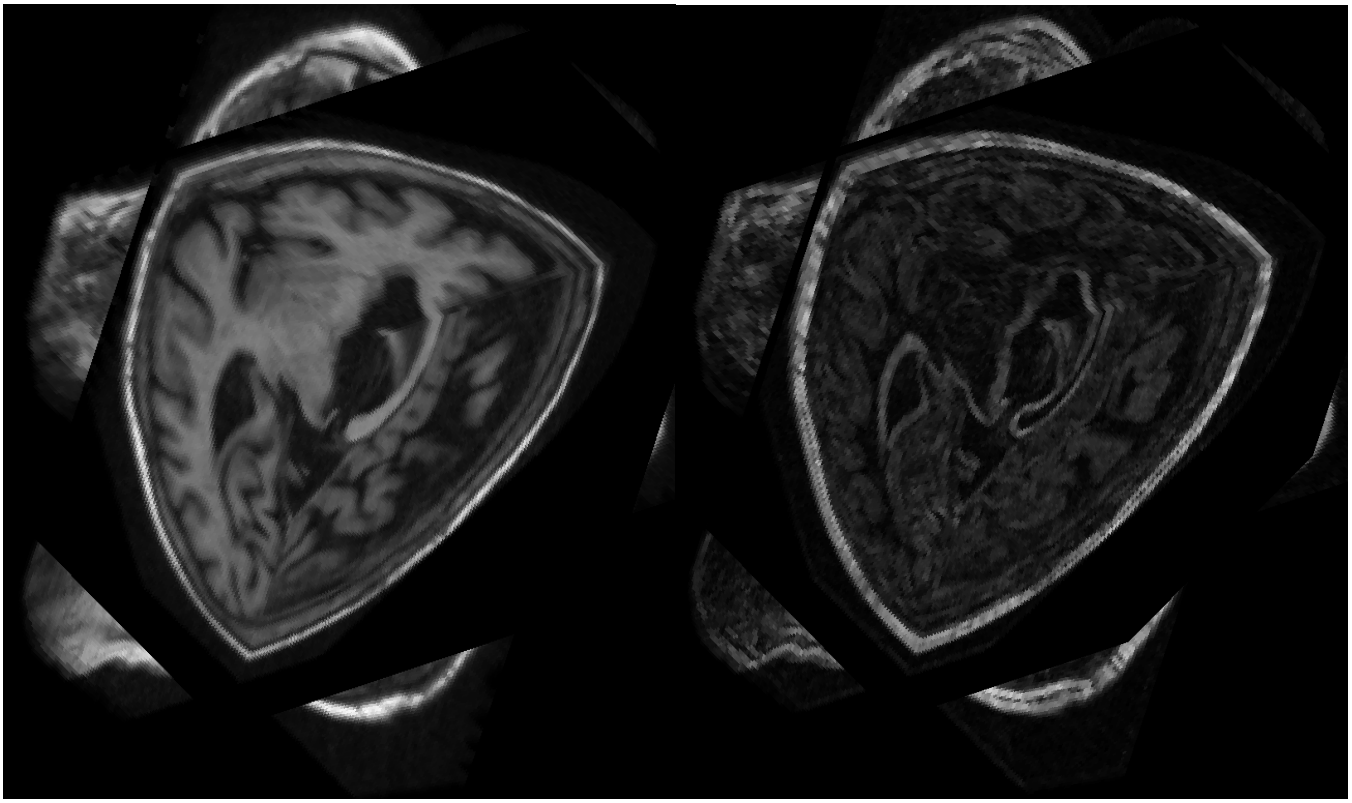

Fig. 3. 3D view showing saggital, coronal, and transverse sections through the third ventricle. Left: Image with intensity values as provided in the data. Right: Intensity values calculated by the difference in intensity between each voxel and 6 non-diagonal neighbors.

subgraphs are found even if the support threshold was high enough to require all 27 trees to contain every subgraph.

Subdue [3] attempts to find subgraphs which are frequent in positive examples, but not negative examples. This is an essential capability for classification of trees derived from the shape of the third ventricle, because it generates a small but relevant set of frequent subgraphs. In order to generate a more diverse set of subgraphs, Subdue was run twice, once with the labels reversed, to find subgraphs which are frequent in negative examples but not positive examples. Subdue is also capable of running in multiple iterations, to find a set of subgraphs which were not covered by frequent subgraphs discovered in earlier iterations. This capability was used provided computational time was available. Some experiments were performed on a cluster with a 24-hour maximum walltime limit, which restricted the maximum time Subdue could be allowed to run. An MPI version of Subdue exists which may ease this requirement somewhat, but this was not used for the present work.

Once a set of subgraph features is obtained, a binary feature vector is created for each example based on the presence or absence of each subgraph. Length is adjustable based on the number of subgraph featuress considered. For most tests, length was between 6 and 100. Subgraphs can be pruned by removing subgraphs which are unlikely to be generally useful, as defined by those not containing a root node. Such substructures appear useful in the training set, but may not apply in general. All substructures not containing the root node are eliminated, because these do not contain any relevant spacial information (i.e. could occur in any part of the graph). This does prevent consideration of local features which are meaningful regardless of location.

Subdue includes a utility called ”cvtest” which can perform classification, although it does not support classification based on subgraphs obtained by reversing the data labels. This utility was used for initial tests. However, it performs subgraph isomorphism to determine which subgraphs are contained in each test example, which is an NP-hard operation and proved very slow on the large (average 2167-node) trees. An attempt to quantify the time required was abandoned after several days.

Given that the non-root-containing substructures have been eliminated, there is no need for an NP-hard isomorphism test. Instead, starting at the root node in the subgraph, all branches are matched to branches in the potential supergraph. Assuming all match, the process is repeated recursively for each branch, avoiding backtracking back up the tree. This allows efficient isomorphism testing. Algorithm 2 describes this in detail. The final classification system was very fast except for substructure discovery, can incorporate an arbitrary number of subgraphs as features, and allows for additional features to be added.

Once a feature vector is constructed, many common machine learning methods can be used. In this work, a Support Vector Machine with an RBF kernel was chosen, as described in [16]. The specific SVM implementation was libsvm [17]. Classification accuracy was found to depend more on the subgraph discovery step than on the particular method of feature vector classification.

An example of a frequent subtree is given in figure 4.

Algorithm 2: Fast test to determine if one tree contains another, exploiting the fact that both trees contain only one root

Input: Candidate supergraph G with root R_G and visited nodes P_G (P_G initially empty), subgraph s with root R_s and visited nodes P_s (P_s initially empty)

Output: true if s is a subgraph of G

INTREE(G, R_G, P_G, s, R_s, P_s)

(1) $N_G \leftarrow$ Neighbors of R_G not in P_G
(2) $N_s \leftarrow$ Neighbors of R_s not in P_s
(3) **foreach** $n \in N_s$
(4) **if** No match for n in N_G
(5) **return false**
(6) **foreach** $n \in N_s$
(7) $n_G \leftarrow$ match for n in G
(8) **if true** $\neq$ intree(G, n_G, $P_G + n_G$, s, n, $P_s + n$)
(9) **return false**
(10) **return true**

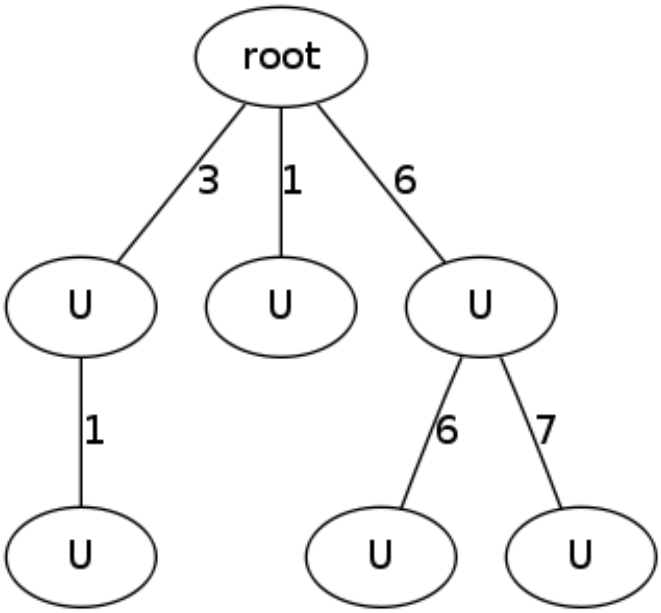

Fig. 4. Frequent subtree from the initial testing set (54 individuals, 27 CDR 1 or higher, 27 CDR 0). This tree appears in 25 positive (CDR $\geq$ 1) examples, and only 5 negative (CDR = 0) examples. Edge 6 from the root leads to a node with two children, representing the left superior portion of the left superior rostral subdivision. Uneven coloration of this area indicates that it is not firmly outside the ventricular system.

VI. Results

In the set of trees created to represent images in the OASIS, trees were limited to a maximum depth of 5, giving a theoretical maximum graph size of 8^5 nodes, or 32,768. The average case was 2,167 nodes. The maximum tree size was well below the theoretical peak at 3,913 nodes. Minimum graph size was 169 nodes. This proved to be a reasonable balance of computational feasibility and accurate representation of the ventricles. Once an appropriate set of graphs was generated, it was not modified for the remainder of the tests.

The initial dataset size was 54, evenly split between healthy individuals and individuals with a CDR of 1 or greater. A complete test using 10-fold cross-validation can be completed on this dataset in about 24 hours, using a 4-core Intel Q6600 CPU and multithreading by performing each fold of cross-validation in its own thread. Results on this dataset indicate an overall accuracy of 72% using 10-fold cross-validation, and 88% accuracy testing on the training set. This dataset omits individuals with CDR 0.5, which is expected to improve accuracy.

Cross-validation is expected to produce lower accuracy than testing on the training set. In this case, the extra error is due to the subgraph mining phase of classification. This was determined by creating a set of feature vectors providing the subgraph miner with complete access to the dataset. Then, accuracy of a Support Vector Machine was obtained over the set of feature vectors using 10-fold cross-validation. This produced 88% accuracy, equivalent to that produced by testing on the training set. A Naive Bayes classifier used on the feature vectors generated a similar result. If appropriate features can be determined by frequent subgraph mining, the machine learning task is then relatively easy.

In order to include individuals with CDR 0.5, a dataset consisting of 83 healthy individuals and 83 individuals with CDR of at least 0.5 was constructed. 10-fold cross-validation test on this dataset can be completed in under 24 hours using 10 Intel Xenon processors running at 2.3 ghz, running each fold of cross-validation on its own processor. Overall accuracy was 66.3%, indicating that inclusion of individuals displaying a lower level of cognitive impairment does increase the difficulty of the learning task, but at least some degree of accuracy is still possible. Given the flexibility of the human brain, it is possible that one could exhibit adequate physical symptoms more strongly than an evaluation of cognitive functioning would indicate, making the slightly-impaired case much more difficult.

Other studies have focused on assessing the progression of Alzheimer's disease, rather than initial assessment of it [2]. There does not appear to be a benchmark classification system to compare ours to, and as such, we have not included results from any other classification system.

A. Level of Education

Given results such as [2], it was expected that some correlation between ventricle shape and level of cognitive impairment exists. However, in addition to CDR, the OASIS dataset contains other parameters, one of which is level of education. Level of education is given as integers from 0 through 5 representing the number of years of education the individual has received [12], with 181 of the total 416 individuals at level 0.

In order to test the classifier, a dataset was constructed using as one category level 0 individuals, and as the other individuals with level 4 or higher. The dataset was balanced with 79 examples of each category. Overall accuracy using 10-fold cross-validation was 77.2%. The accuracy proved insensitive to adjustments in the RBF kernel parameters C and γ. Accuracy decreased if the parameters were set very high in order to overfit the data, however for all reasonable settings

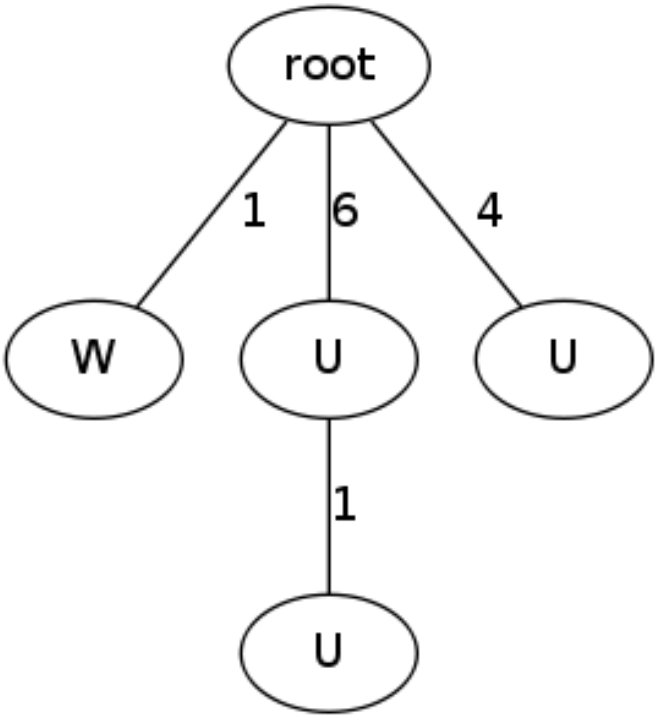

Fig. 5. Frequent subtree from the education test set. This tree is present in 42 examples with individuals having 4 or more years of college education, but only 7 examples of individuals with no college education. Note that the right inferior caudal subdivision is found to be white. This may indicate small overall ventricular size, because if the ventricles were large, this area would not be completely outside the ventricular system.

accuracy was unchanged. This emphasizes the result that subgraph discovery is more important to accurate classification than the method used to classify feature vectors. An example frequent subtree is given in figure 5.

From this, it may be concluded that there is a correlation between the shape of the third and lateral ventricles and the level of education a person has received, at least in the tested images from the OASIS database. This does not imply any particular causation, merely that the correlation exists to such an extent that a computer program can use the shape of the ventricles to distinguish between highly-educated people and those with no college education nearly 4 out of every 5 times.

There are examples in the literature regarding the effect of education on the brain. For example, in [18], it is noted that years of education results in higher performance on intelligence tests into old age. It is also discovered that although higher initial performance is observed, verbal memory performance may decline faster on well-educated subjects.

In [19] more rapid cognitive decline due to Alzheimer's disease on highly-educated test subjects is observed. A peculiarity of the OASIS dataset is that all cognitively-impaired individuals had at least a year of higher education. The total number of subjects with at least 1 year of higher education is 235, of which 100 have CDR ≥ 0.5.

We are not aware of any previous work that specifically correlates ventricular size or shape to level of education.

VII. Future Work

The graph-based 3D shape classification described in this paper is intended to be readily incorporated into a more expansive graph of the brain. A number of methods presently exist to form a graph representing neural structure.

Eguíluz et al. use functional MRI activation levels in order to link areas of the brain with correlated activation in [20]. This produces a graph where two nodes are linked if the areas they represent activate at the same times. This is considered to be a functional brain network [21].

A different approach is taken by Hagmann et al. in [22]. A graph is formed of the structure of the brain, indicating which neural component is connected to which other neural component by analysis of white matter. This forms a structural brain network [21].

Both structural and functional networks could be suitable for graph-based classification as done in this paper. However, the state of the brain could be more completely described by incorporating shape-based information into the graph. Using trees to represent the 3D shape of neural components is a natural method for this. The root of the shape tree for a neural structure can be linked to the node representing that structure. A frequent subgraph based classifier could directly process the resulting graph. Such a graph would incorporate far more information than the graphs of the ventricles, and the shape of the graph is likely to correlate with more conditions. In essence, this would produce a more generally useful version of the system described in this paper.

Besides providing an automatic method of distinguishing between categories of brain images, such a system could provide a insight into what physical differences are important in recognizing the condition. Frequent subgraphs useful to classification will incorporate nodes from relevant structures, but not structures which have no bearing on the eventual classification.

A. Robustness of the Method

The ventricle discovery algorithm was able to process 387 out of 416 images. Of the remainder, most had severely enlarged ventricles which resulted in discovery of the cerebral aquaduct and fourth ventricle. A few had small ventricular systems, with no clear passage between the third ventricle and the lateral ventricles. In either case, manual analysis would readily reveal the state of the ventricular system. A replacement ventricle discovery system based on image analysis techniques may be able to improve upon this.

VIII. Conclusion

This work was intended to validate the hypothesis that a graph-based representation of the 3D shape of the third and lateral ventricle would enable a graph classifier to distinguish between MR images of brains in patients with cognitive impairment due to Alzheimer's disease and healthy patients. It can do that to some degree, even when mildly-impaired patients are included in the dataset. The method also proved suitable to distinguish highly-educated individuals from those with no college education. This demonstrates the versatility of

the solution, and also provides the interesting result that at least in the OASIS dataset, there is a significant difference in the shape of the third and lateral ventricles between these groups. We are aware of no previous study correlating ventricular size with level of education, although the role of education in cognitive decline has been previously studied.

Given this, a more general system incorporating more neural structures than just the ventricular system is likely to be of at least some utility in detecting a variety of neural conditions, and also of finding the physical differences which make them distinguishable. The graph-based shape recognition algorithm could play a key role in such a system.

REFERENCES

[1] V. Megalooikonomou, J. Ford, L. Shen, F. Makedon, and A. Saykin, "Data mining in brain imaging," *Statistical Methods in Medical Research*, vol. 9, no. 4, p. 359, 2000.

[2] S. Nestor, R. Rupsingh, M. Borrie, M. Smith, V. Accomazzi, J. Wells, J. Fogarty, and R. Bartha, "Ventricular enlargement as a possible measure of alzheimer's disease progression validated using the alzheimer's disease neuroimaging initiative database," *Brain*, vol. 131, no. 9, p. 2443, 2008.

[3] D. J. Cook and L. B. Holder, "Graph-based data mining," *IEEE Intelligent Systems*, vol. 15, no. 2, pp. 32–41, 2000.

[4] M. Deshpande, M. Kuramochi, N. Wale, and G. Karypis, "Frequent substructure-based approaches for classifying chemical compounds," *IEEE Transactions on Knowledge and Data Engineering*, vol. 17, no. 8, pp. 1036–1050, 2005.

[5] T. Gaertner, P. Flach, and S. Wrobel, "On graph kernels: Hardness results and efficient alternatives," in *Proceedings of the 16th Annual Conference on Computational Learning Theory and 7th Kernel Workshop*. Springer-Verlag, August 2003, pp. 129–143. [Online]. Available: http://www.cs.bris.ac.uk/Publications/Papers/2000555.pdf

[6] S. Long and L. Holder, "Using graphs to improve activity prediction in smart environments based on motion sensor data," in *Towards Useful Services for Elderly and People with Disabilities: 9th International Conference on Smart Homes and Health Telematics, ICOST 2011, Montreal, Canada, June 20-22, 2011, Proceedings*, vol. 6719. Springer, 2011, p. 57.

[7] S. Joshi and T. Chang, "Graph-based heuristics for recognition of machined features from a 3d solid model," *Computer-Aided Design*, vol. 20, no. 2, pp. 58–66, 1988.

[8] C. de Mauro, M. Diligenti, M. Gori, and M. Maggini, "Similarity learning for graph-based image representations," *Pattern Recognition Letters*, vol. 24, no. 8, pp. 1115–1122, 2003.

[9] A. Elsayed, F. Coenen, C. Jiang, M. García-Fiñana, and V. Sluming, "Corpus callosum MR image classification," *Knowledge-Based Systems*, vol. 23, no. 4, pp. 330–336, 2010.

[10] A. Elsayed, F. Coenen, M. Garcia-Fiñana, and V. Sluming, "Region of interest based image classification using time series analysis," in *Neural Networks (IJCNN), The 2010 International Joint Conference on*. IEEE, 2010, pp. 1–6.

[11] T. Mitchell, R. Hutchinson, R. Niculescu, F. Pereira, X. Wang, M. Just, and S. Newman, "Learning to decode cognitive states from brain images," *Machine Learning*, vol. 57, no. 1, pp. 145–175, 2004.

[12] D. Marcus, T. Wang, J. Parker, J. Csernansky, J. Morris, and R. Buckner, "Open Access Series of Imaging Studies (OASIS): cross-sectional MRI data in young, middle aged, nondemented, and demented older adults," *Journal of Cognitive Neuroscience*, vol. 19, no. 9, pp. 1498–1507, 2007.

[13] K. Millman and M. Brett, "Analysis of functional magnetic resonance imaging in Python," *Computing in Science & Engineering*, pp. 52–55, 2007.

[14] S. Nijssen and J. N. Kok, "A quickstart in frequent structure mining can make a difference," in *KDD '04: Proceedings of the tenth ACM SIGKDD international conference on Knowledge discovery and data mining*. New York, NY, USA: ACM, 2004, pp. 647–652.

[15] X. Yan and J. Han, "gSpan: graph-based substructure pattern mining," in *Data Mining, 2002. ICDM 2002. Proceedings. 2002 IEEE International Conference on*. IEEE, 2002, pp. 721–724.

[16] K. Muller, S. Mika, G. Ratsch, K. Tsuda, and B. Scholkopf, "An introduction to kernel-based learning algorithms," *IEEE transactions on neural networks*, vol. 12, no. 2, pp. 181–201, 2001.

[17] C.-C. Chang and C.-J. Lin, *LIBSVM: a library for support vector machines*, 2001, software available at http://www.csie.ntu.edu.tw/ cjlin/libsvm.

[18] D. Alley, K. Suthers, and E. Crimmins, "Education and cognitive decline in older americans," *Research on aging*, vol. 29, no. 1, p. 73, 2007.

[19] R. Wilson, Y. Li, N. Aggarwal, L. Barnes, J. McCann, D. Gilley, and D. Evans, "Education and the course of cognitive decline in alzheimer disease," *Neurology*, vol. 63, no. 7, p. 1198, 2004.

[20] V. Eguiluz, D. Chialvo, G. Cecchi, M. Baliki, and A. Apkarian, "Scale-free brain functional networks," *Physical Review Letters*, vol. 94, no. 1, p. 18102, 2005.

[21] E. Bullmore and O. Sporns, "Complex brain networks: graph theoretical analysis of structural and functional systems," *Nature Reviews Neuroscience*, vol. 10, no. 3, pp. 186–198, 2009.

[22] P. Hagmann, M. Kurant, X. Gigandet, P. Thiran, V. Wedeen, R. Meuli, and J. Thiran, "Mapping human whole-brain structural networks with diffusion MRI," *PLoS One*, vol. 2, no. 7, p. 597, 2007.